Recent results on correlations and fluctuations in pp, p+Pb, and Pb+Pb collisions from the ATLAS experiment at the LHC

Mariusz Przybycień

AGH University of Science and Technology, Krakow, Poland

(on behalf of the ATLAS Collaboration)

Recent ATLAS results to be reviewed in this talk

- Measurement of multi-particle azimuthal correlations in pp, p+Pb and low-multiplicity Pb+Pb collisions with the ATLAS detector. Eur. Phys. J. C (2018) 77:428
- Measurement of long-range multiparticle azimuthal correlations with the subevent cumulant method in pp and p+Pb collisions with the ATLAS detector at the LHC. Phys. Rev. C 97, 024904 (2018)
- Correlated long-range mixed-harmonic fluctuations in pp, p+Pb and low-multiplicity Pb+Pb collisions with the ATLAS detector. ATLAS-CONF-2018-012
- Measurement of long-range azimuthal correlations in Z-boson tagged pp collisions at $\sqrt{s} = 8$ TeV. ATLAS-CONF-2017-068
- D meson production and long-range azimuthal correlations in 8.16 TeV p+Pb collisions with ATLAS. ATLAS-CONF-2017-073
- Measurement of longitudinal flow decorrelations in Pb+Pb collisions at $\sqrt{s_{\mathrm{NN}}} = 2.76$ and 5.02 TeV with the ATLAS detector. Eur. Phys. J. C (2018) 78:142
- Measurement of the $\mathrm{v}_n -$ mean p_{T} correlations in Pb+Pb collisions at $\sqrt{s_{\mathrm{NN}}} = 5.02$ TeV with the ATLAS detector. ATLAS-CONF-2018-008
- Measurement of azimuthal anisotropy of charged particle production in Xe+Xe collisions at $\sqrt{s_{\mathrm{NN}}} = 5.44$ TeV with the ATLAS detector. ATLAS-CONF-2018-011
- More details and results from the heavy ion physics program realized by ATLAS are available in https://twiki.cern.ch/twiki/bin/view/AtlasPublic/HeavyIonsPublicResults

Introduction

- Immadiately after an A+A collision, the overlap region defined by the nuclear geometry is almond shaped, with shortest axis along the impact parameter vector.
- Multiple interactions between particles in the evolving system change the initial coordinate space asymmetry into final momentum space asymmetry.

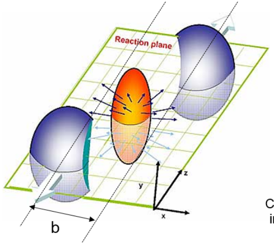

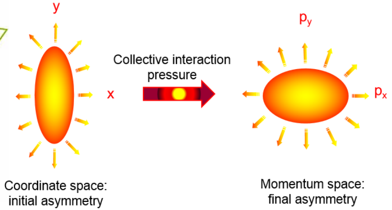

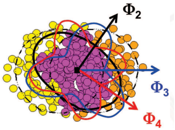

Φ_n - azimuthal angle of the n-th order symmetry plane of the initial geometry,

$$E\frac{\mathrm{d}^3N}{\mathrm{d}p^3} = \frac{1}{p_\mathrm{T}}\frac{\mathrm{d}^3N}{\mathrm{d}\phi\,\mathrm{d}p_\mathrm{T}\,\mathrm{d}y} = \frac{1}{2\pi p_\mathrm{T}}\frac{E}{p}\frac{\mathrm{d}^2N}{\mathrm{d}p_\mathrm{T}\,\mathrm{d}\eta}\left(1 + 2\sum_{n=1}^{\infty}\mathrm{v}_n(p_\mathrm{T},\eta)\cos\left(n(\phi-\Phi_n)\right)\right)$$

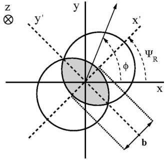

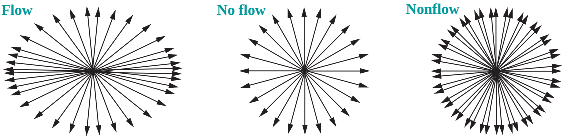

Two-particle correlations and the template fitting method

- Two-particle correlation function (and focus on LRC):

$$C(\Delta\eta,\Delta\phi)=\frac{S(\Delta\eta,\Delta\phi)}{B(\Delta\eta,\Delta\phi)}\ \xrightarrow[\int_2^5 \mathrm{d}|\Delta\eta|]{\int_2^5 \mathrm{d}|\Delta\eta|}\ \frac{S(\Delta\phi)}{B(\Delta\phi)}\equiv C(\Delta\phi)$$

  - S and B are pair distributions constructed from the same and from "mixed events" (similar $N_{\mathrm{ch}}^{\mathrm{rec}}$ and z_{vtx}).
  - Ratio S/B removes correlations due to detector effects.

- Per-trigger-particle yield - the average number of associated particles per trigger particle in a given $\Delta\phi$ range:

$$Y(\Delta\phi)=\frac{1}{2\pi}\frac{1}{N^{\mathrm{trig}}}\left(\int_{-\pi/2}^{3\pi/2}B(\Delta\phi)\mathrm{d}\Delta\phi\right)C(\Delta\phi)$$

- Template fitting procedure is applied to separate ridge from other sources of angular correlations (e.g. dijets):

$$Y^{\mathrm{templ}}(\Delta\phi)=\underbrace{G\left(1+\sum_{n=2}^{\infty}2\mathrm{v}_{n,n}\cos(n\Delta\phi)\right)}_{Y^{\mathrm{ridge}}}+F\,Y^{\mathrm{periph}}(\Delta\phi)$$

  where $Y^{\mathrm{periph}}(\Delta\phi)$ is obtained from low-multiplicity events.

- Importance of higher order harmonics is also visualized.

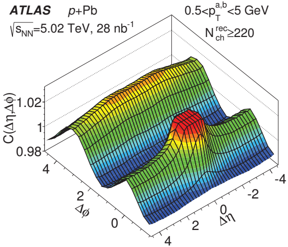

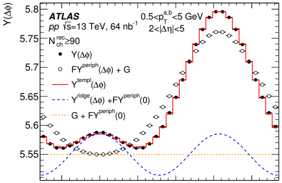

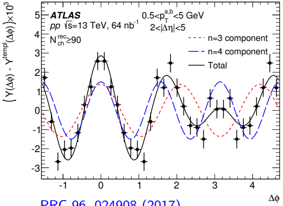

PRC 96, 024908 (2017)

Cumulants with the standard method

- The standard cumulant method is based on the k-particle azimuthal correlations, $\langle\{k\}\rangle$:

$$\langle\{2\}_n\rangle = \left\langle e^{in(\phi_1-\phi_2)}\right\rangle, \quad \langle\{3\}_n\rangle = \left\langle e^{in(\phi_1+\phi_2-2\phi_3)}\right\rangle, \quad \langle\{4\}_{n,m}\rangle = \left\langle e^{in(\phi_1-\phi_2)+im(\phi_3-\phi_4)}\right\rangle$$

- The 2- and 4-particle cumulants are than defined as:

$$c_n\{2\} = \langle\langle\{2\}_n\rangle\rangle, \qquad c_n\{4\} = \langle\langle\{4\}_n\rangle\rangle - 2\langle\langle\{2\}_n\rangle\rangle^2 \quad \text{where} \quad \langle\{4\}_n\rangle \equiv \langle\{4\}_{n,n}\rangle$$

- The multi-particle symmetric and asymmetric cumulants are obtained from $\langle\{k\}\rangle$ as:

$$ac_n\{3\} = \langle\langle\{3\}_n\rangle\rangle, \quad sc_{n,m}\{4\} = \langle\langle\{4\}_{n,m}\rangle\rangle - \langle\langle\{2\}_n\rangle\rangle\langle\langle\{2\}_m\rangle\rangle$$

- In the absence of non-flow correlations, $c_n\{2\}$, $c_n\{4\}$, $ac_n\{3\}$ and $sc_{n,m}\{4\}$ read:

$$c_n\{2\} = \mathrm{v}_n^2, \quad c_n\{4\} = -\mathrm{v}_n^4, \quad sc_{n,m}\{4\} = \langle \mathrm{v}_n^2\mathrm{v}_m^2\rangle - \langle\mathrm{v}_n^2\rangle\langle\mathrm{v}_m^2\rangle$$

$$ac_n\{3\} = \langle \mathrm{v}_n^2 \mathrm{v}_{2n}\cos 2n(\Phi_n - \Phi_{2n})\rangle$$

- Normalized cumulants:

$$nsc_{n,m}\{4\} = \frac{sc_{n,m}\{4\}}{\mathrm{v}_n\{2\}^2\mathrm{v}_m\{2\}^2} = \frac{\langle \mathrm{v}_n^2\mathrm{v}_m^2\rangle}{\langle\mathrm{v}_n^2\rangle\langle\mathrm{v}_m^2\rangle} - 1$$

$$nac_n\{3\} = \frac{ac_n\{3\}}{\mathrm{v}_n\{2\}^2\sqrt{\mathrm{v}_{2n}\{2\}^2}} = \frac{\langle \mathrm{v}_n^2\mathrm{v}_{2n}\cos 2n(\Phi_n - \Phi_{2n})\rangle}{\langle\mathrm{v}_n^2\rangle\sqrt{\langle\mathrm{v}_{2n}^2\rangle}}$$

where the $\mathrm{v}_n\{2\}^2 = \langle\mathrm{v}_n^2\rangle$ are flow harmonics obtained using a 2-particle correlation method based on the template fitting method.

Cumulants with the subevent method (SE)

To suppress the non-flow correlations, that usually involve few particles within a localized region in η, the tracks are divided into several subevents, each covering a unique η range. Multi-particle correlations are constructed by correlating tracks from different subevents.

- Two subevents (2SE) - removes intra-jet correlations

$$\langle\{2\}_n\rangle_{a|b} = \left\langle e^{in(\phi_1^a-\phi_2^b)}\right\rangle \qquad sc_{n,m}^{2a|2b}\{4\} = \langle\langle\{4\}_{n,m}\rangle\rangle_{2a|2b} - \langle\langle\{2\}_n\rangle\rangle_{a|b}\langle\langle\{2\}_m\rangle\rangle_{a|b}$$

$$\langle\{3\}_n\rangle_{2a|b} = \left\langle e^{in(\phi_1^a+\phi_2^a-2\phi_3^b)}\right\rangle \qquad ac_n^{2a|b}\{3\} = \langle\langle\{3\}_n\rangle\rangle_{2a|b} \qquad c_n^{a|b}\{2\} = \langle\langle\{2\}_n\rangle\rangle_{a|b}$$

$$\langle\{4\}_{n,m}\rangle_{2a|2b} = \left\langle e^{in(\phi_1^a-\phi_2^b)+im(\phi_3^a-\phi_4^b)}\right\rangle \qquad c_n^{2a|2b}\{4\} = \langle\langle\{4\}_n\rangle\rangle_{2a|2b} - 2\langle\langle\{2\}_n\rangle\rangle_{a|b}^2$$

- Three subevents (3SE) - removes inter-jet correlations

$$\langle\{3\}_n\rangle_{a,b|c} = \left\langle e^{in(\phi_1^a+\phi_2^b-2\phi_3^c)}\right\rangle \qquad sc_{n,m}^{a,b|2c}\{4\} = \langle\langle\{4\}_{n,m}\rangle\rangle_{a,b|2c} - \langle\langle\{2\}_n\rangle\rangle_{a|c}\langle\langle\{2\}_m\rangle\rangle_{b|c}$$

$$\langle\{4\}_{n,m}\rangle_{a,b|2c} = \left\langle e^{in(\phi_1^a-\phi_2^c)+im(\phi_3^b-\phi_4^c)}\right\rangle \qquad ac_n^{a,b|c}\{3\} = \langle\langle\{3\}_n\rangle\rangle_{a,b|c}$$

$$c_n^{a,b|2c}\{4\} = \langle\langle\{4\}_n\rangle\rangle_{a,b|2c} - \langle\langle\{2\}_n\rangle\rangle_{a|c}\langle\langle\{2\}_n\rangle\rangle_{b|c}$$

- Four subevents (4SE) - removes partly inter-jet correlations also in case of jets belonging to two adjacent subevents

$$\langle\{4\}_{n,m}\rangle_{a,b|c,d} = \left\langle e^{in(\phi_1^a-\phi_2^c)+im(\phi_3^b-\phi_4^d)}\right\rangle$$

$$sc_{n,m}^{a,b|c,d}\{4\} = \langle\langle\{4\}_{n,m}\rangle\rangle_{a,b|c,d} - \langle\langle\{2\}_n\rangle\rangle_{a|c}\langle\langle\{2\}_m\rangle\rangle_{b|d}$$

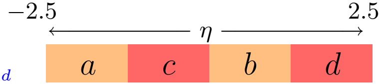

$c_2\{4\}$ cumulant and v_2 in pp and p+Pb with SE method

- The $c_2\{4\}$ values in pp collisions and in p+Pb collisions for $\langle N_{\mathrm{ch}}\rangle < 100$ are smallest for the 3SE method and largest for the standard method.
- In the p+Pb collisions the $c_2\{4\}$ are consistent for all three methods for $\langle N_{\mathrm{ch}}\rangle > 100$ sugesting that non-flow effects in p+Pb colisions are much smaller than those in pp collisions at comparable $\langle N_{\mathrm{ch}}\rangle$.
- The 3SE method gives negative $c_2\{4\}$ values in most of the measured $\langle N_{\mathrm{ch}}\rangle$ range.
- The $\mathrm{v}_2\{4\}$ values obtained from the 3SE method are smaller than $\mathrm{v}_2\{2\}$ extracted from 2PC, possibly due to EbyE flow fluctuations associated with the initial state (PRL 112, 082301 (2014)).

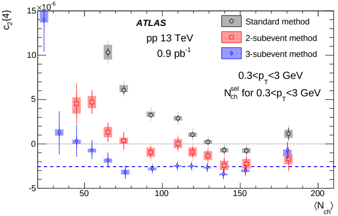

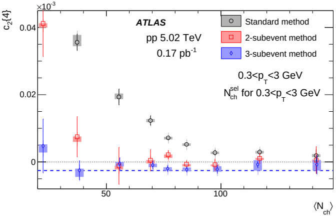

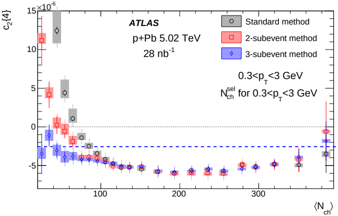

PRC 97, 024904 (2018)

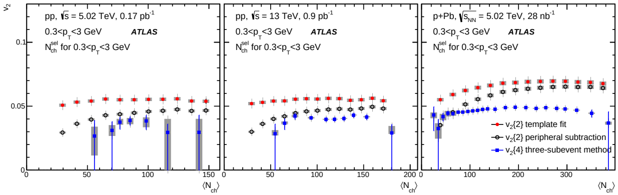

Symmetric cumulant $sc_{2,3}\{4\} = \langle v_2^2 v_3^2 \rangle - \langle v_2^2 \rangle \langle v_3^2 \rangle$

- Measured in two p_{T} intervals: $0.3 < p_{\mathrm{T}} < 3$ GeV and $0.5 < p_{\mathrm{T}} < 5$ GeV.
- In pp and at low values of $\langle N_{\mathrm{ch}} \rangle$ in p+Pb the $sc_{2,3}\{4\}$ obtained from the standard method are positive and significantly differ from SE.
- Non-flow is largely suppressed in SE; some residual non-flow in pp at low $\langle N_{\mathrm{ch}} \rangle$ in 2SE.
- For the p_{T} region of $0.5 < p_{\mathrm{T}} < 5$ GeV results from 2SE are systematically lower than the 3SE/4SE, suggesting that the 2SE method my be affected by negative non-flow contribution (recently observed in PYTHIA, PLB777 (2018) 201).
- Anticorrelation between v_2 and v_3 in SE.
- In case of Pb+Pb collisions the measured $sc_{2,3}\{4\}$ is consistent among all four methods across most of the $\langle N_{\mathrm{ch}} \rangle$ range.
- 3SE method seems to be good enough for non-flow removal.

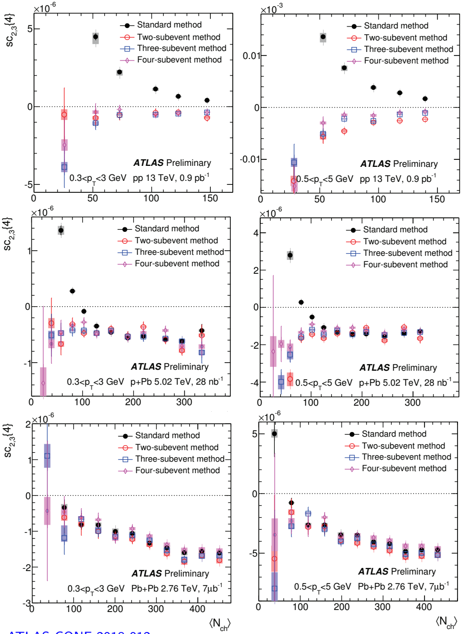

ATLAS-CONF-2018-012

Symmetric cumulant $sc_{2,4}\{4\} = \langle v_2^2 v_4^2 \rangle - \langle v_2^2 \rangle \langle v_4^2 \rangle$

- Measured in two p_T intervals: $0.3 < p_T < 3$ GeV and $0.5 < p_T < 5$ GeV.
- In pp and in p+Pb the $sc_{2,4}\{4\}$ obtained from the standard method are positive and significantly differ from SE methods.
- Non-flow is largely suppressed in SE; some residual non-flow in pp at low $\langle N_{ch} \rangle$ in 2SE.
- Positive correlation between v_2 and v_4 is observed in all methods due to non-linear effect $v_4 = v_{4L} + \chi^2 v_2^2$.
- In case of Pb+Pb collisions the measured $sc_{2,4}\{4\}$ is consistent among all SE methods while the standard method gives values systematically larger.
- 3SE method seems to be good enough for non-flow removal.

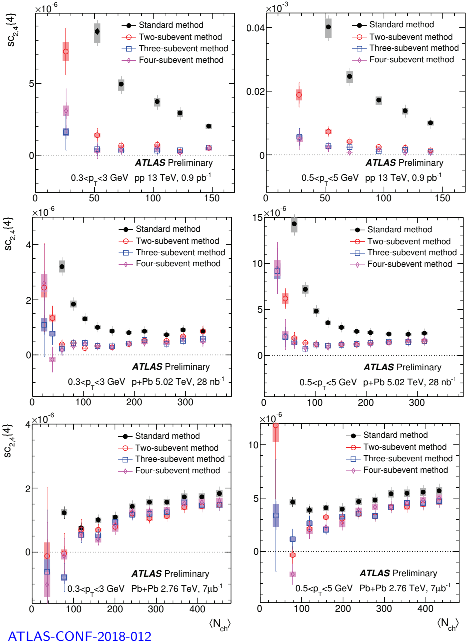

ATLAS-CONF-2018-012

Asymmetric cumulant $ac_2\{3\} = \langle v_2^2 v_4 \cos 4(\Phi_2 - \Phi_4)\rangle$

- Measured in two p_T intervals: $0.3 < p_T < 3$ GeV and $0.5 < p_T < 5$ GeV.
- The $ac_2\{3\}$ are positive for all methods.
- The standard method gives much larger results then the SE methods $\Rightarrow$ standard method is dominated by non-flow effects.
- The $ac_2\{3\}$ from the 3SE method in pp collisions show some increase at low $\langle N_{ch}\rangle$, but are nearly constant at large $\langle N_{ch}\rangle$. This suggest that 3SE method contains some non-flow contribution at $\langle N_{ch}\rangle < 40$ which is negligible at larger $\langle N_{ch}\rangle$.
- In SE methods in both p+Pb and Pb+Pb collisions the influence of non-flow effects is very small for $\langle N_{ch}\rangle > 60$. The $ac_2\{3\}$ from SE increase with $\langle N_{ch}\rangle$ reflecting the $\langle N_{ch}\rangle$ dependence of the v_2 and v_4.
- Difference between standard and SE methods at large $\langle N_{ch}\rangle$ could be due to flow decorelation (EPJC 78 (2018) 142).

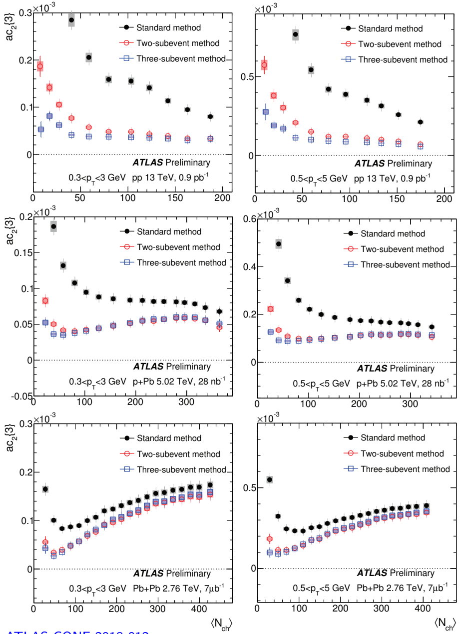

ATLAS-CONF-2018-012

System size dependence

- Use 3SE method as it is sufficient to suppress most of the non-flow effects.
- The results for $sc_{2,3}\{4\}$, $sc_{2,4}\{4\}$ and $ac_2\{3\}$ support in small collision systems, an anti-correlation between v_2 and v_3 and a positive correlation between v_2 and v_4, the pattern observed previously in large collision systems.
- In the multiplicity range covered by the pp collisions, $\langle N_{ch} \rangle < 150$, the $sc_{2,3}\{4\}$ and $sc_{2,4}\{4\}$ are similar among the three systems.
- For $\langle N_{ch} \rangle > 150$, $sc_{2,3}\{4\}$ and $sc_{2,4}\{4\}$ are larger in Pb+Pb than in p+Pb collisions.
- The results for $ac_2\{3\}$ are similar among the three systems at $\langle N_{ch} \rangle < 100$, but they deviate from each other at higher $\langle N_{ch} \rangle$: pp data are approximately constant, while p+Pb and Pb+Pb data show significant increases as a function of $\langle N_{ch} \rangle$.

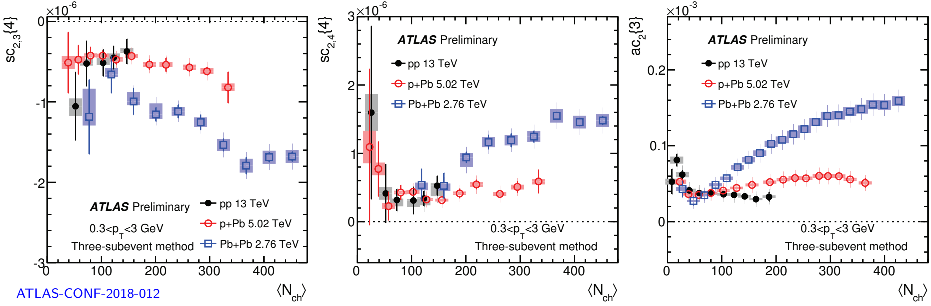

ATLAS-CONF-2018-012

System size dependence

- Use 3SE method as it is sufficient to suppress most of the non-flow effects.
- The results for $sc_{2,3}\{4\}$, $sc_{2,4}\{4\}$ and $ac_2\{3\}$ support in small collision systems, an anti-correlation between v_2 and v_3 and a positive correlation between v_2 and v_4, the pattern observed previously in large collision systems.
- In the multiplicity range covered by the pp collisions, $\langle N_{\mathrm{ch}} \rangle < 150$, the $sc_{2,3}\{4\}$ and $sc_{2,4}\{4\}$ are similar among the three systems.
- For $\langle N_{\mathrm{ch}} \rangle > 150$, $sc_{2,3}\{4\}$ and $sc_{2,4}\{4\}$ are larger in Pb+Pb than in p+Pb collisions.
- The results for $ac_2\{3\}$ are similar among the three systems at $\langle N_{\mathrm{ch}} \rangle < 100$, but they deviate from each other at higher $\langle N_{\mathrm{ch}} \rangle$: pp data are approximately constant, while p+Pb and Pb+Pb data show significant increases as a function of $\langle N_{\mathrm{ch}} \rangle$.

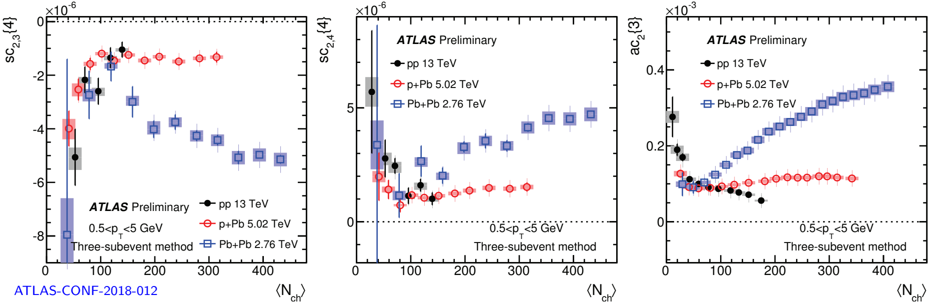

ATLAS-CONF-2018-012

Normalized cumulants

- Remove dependence on harmonics magnitude and focus only on correlation strength.
- Normalization removes most of $\langle N_{\mathrm{ch}} \rangle$ dependence at $\langle N_{\mathrm{ch}} \rangle > 100$.
- Normalized cumulants are similar among different collision systems at large $\langle N_{\mathrm{ch}} \rangle$, although some splitting at the level of $20 - 30\%$ is observed for smaller $\langle N_{\mathrm{ch}} \rangle$.
- Values of $nsc_{2,3}\{4\}$ in pp collisions are very different from those in p+Pb and Pb+Pb collisions. This suggest that the $\langle \mathrm{v}_3^2 \rangle$ values from the template fitting method may be significantly underestimeted.
- Normalized cumulants are consistent between the two p_{T} ranges. These results suggest that p_{T} dependence of symmetric and asymmetric cumulants largely reflects the p_{T} dependence of v_n at the single-particle level.

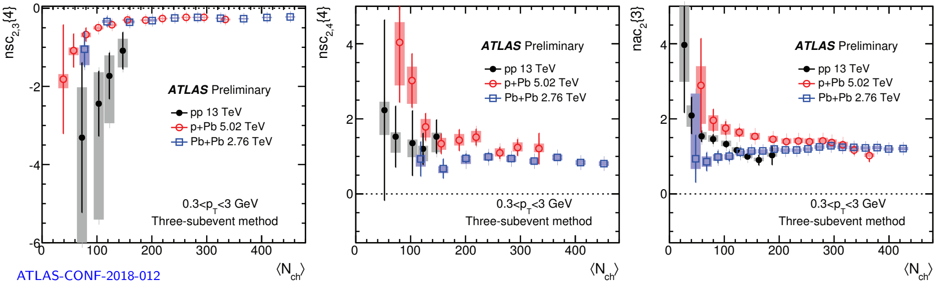

ATLAS-CONF-2018-012

Normalized cumulants

- Remove dependence on harmonics magnitude and focus only on correlation strength.
- Normalization removes most of $\langle N_{\mathrm{ch}} \rangle$ dependence at $\langle N_{\mathrm{ch}} \rangle > 100$.
- Normalized cumulants are similar among different collision systems at large $\langle N_{\mathrm{ch}} \rangle$, although some splitting at the level of $20 - 30\%$ is observed for smaller $\langle N_{\mathrm{ch}} \rangle$.
- Values of $nsc_{2,3}\{4\}$ in pp collisions are very different from those in p+Pb and Pb+Pb collisions. This suggest that the $\langle \mathrm{v}_3^2 \rangle$ values from the template fitting method may be significantly underestimeted.
- Normalized cumulants are consistent between the two p_{T} ranges. These results suggest that p_{T} dependence of symmetric and asymmetric cumulants largely reflects the p_{T} dependence of v_n at the single-particle level.

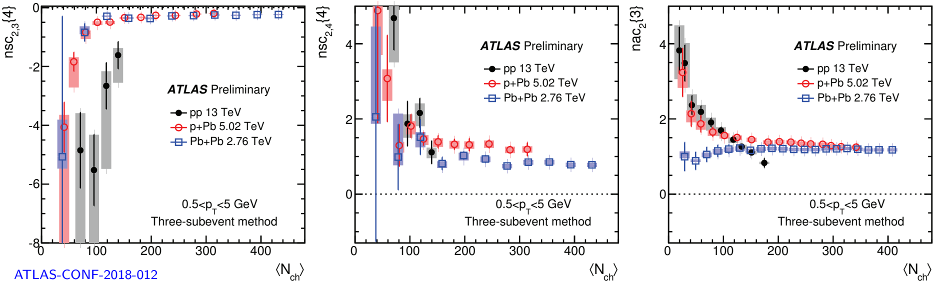

ATLAS-CONF-2018-012

Two-particle correlations in Z-boson tagged pp collisions

- Strong dependence of v_2 on $\langle N_{ch} \rangle$ in p+Pb and Pb+Pb collisions is atributed to the dependence on centrality.
- In pp collisions v_2 is independent of event multiplicity.
- Try to control collision geometry in pp by requiring presence of a Z boson, produced in a hard scattering. Z-boson tagged events have smaller impact parameter b and in consequence smaller v_2 then in inclusive events.
- A new technique was developed to subtract pileup contribution in 2PC measurements.
- A template fitting method was used to extract v_2
- Pileup subtraction changes v_2 by 20% on average.
- Z-tagged v_2 is $8 \pm 6\%$ higher than the inclusive one.
- No multiplicity dependence of v_2 in the Z-tagged data.

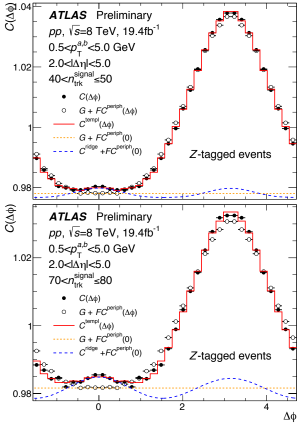

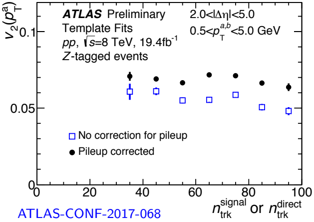

ATLAS-CONF-2017-068

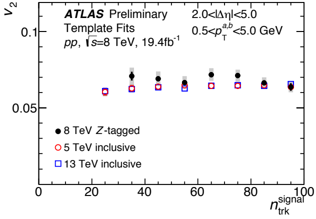

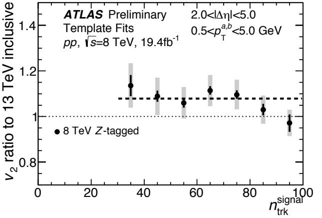

Longitudinal flow decorrelation in Pb+Pb collisions

- Both longitudinal & transverse fluctuation exist in EbyE particle distribution in (η, ϕ). The goal of this analysis is to study the longitudinal flow fluctuation.
- EbyE fluctuation in the magnitude and the phase of the harmonic flow vector:

$\vec{\mathrm{v}}_n(\eta) = \mathrm{v}_n(\eta) e^{in\Phi_n(\eta)}$ is estimated from the observed flow vector $\vec{q}_n \equiv \frac{\sum_i w_i e^{in\phi_i}}{\sum_i w_i}$

- The longitudinal flow fluctuations are studied using the correlation, $r_{n|n;k}$, between the kth-moment of the nth-order flow vectors in two different η intervals, averaged over events in a given centrality interval (sensitive to twist and magnitude decorrelation).
- Another correlator, $R_{n|n;2}$, involving flow vectors in four η intervals is also used to separate contributions of the asymmetry and twist effects.

$$r_{n|n;k}(\eta) = \frac{\langle \vec{q}_n^{\,k}(-\eta)\, \vec{q}_n^{\,\star k}(\eta_{\mathrm{ref}}) \rangle}{\langle \vec{q}_n^{\,k}(\eta)\, \vec{q}_n^{\,\star k}(\eta_{\mathrm{ref}}) \rangle}$$

$$R_{n|n;2}(\eta) = \frac{\langle \vec{q}_n(-\eta_{\mathrm{ref}})\, \vec{q}_n^{\,\star}(\eta)\, \vec{q}_n(-\eta)\, \vec{q}_n^{\,\star}(\eta_{\mathrm{ref}}) \rangle}{\langle \vec{q}_n(-\eta_{\mathrm{ref}})\, \vec{q}_n^{\,\star}(-\eta) \langle \vec{q}_n(\eta)\, \vec{q}_n^{\,\star}(\eta_{\mathrm{ref}}) \rangle}$$

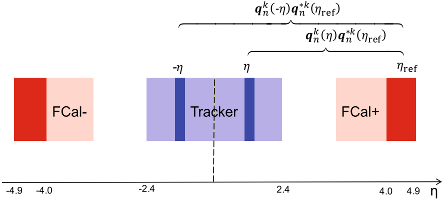

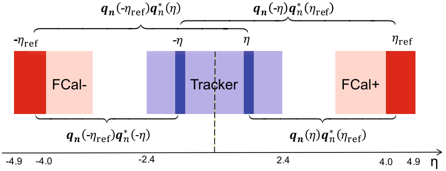

Longitudinal flow decorrelation in Pb+Pb collisions

- $r_{2|2;1}$ shows a linear decrease with η, except in the most central collisions.
- The decreasing trend is weakest around the $20-30\%$ centrality range, and is more pronounced in both more central and more peripheral collisions (related to a strong centrality dependence of the v_2 associated with the average elliptic geometry).
- The decreasing trend is slightly stronger at $\sqrt{s_{\mathrm{NN}}} = 2.76$ TeV than at $\sqrt{s_{\mathrm{NN}}} = 5.02$ TeV collisions(collision system less boosted at lower collision energy).
- Similar linear decrese of $r_{n|n;1}$ with η also for $n = 3, 4$, which is almost independent of centrality ($\mathrm{v}_n,\ n = 3, 4$ are mainly driven by fluctuations in the initial state).
- The decreasing trend of $r_{n|n;1}$ for $n = 2-4$ indicates significant breakdown of the factorisation of two-particle flow harmonics into those between different η ranges.

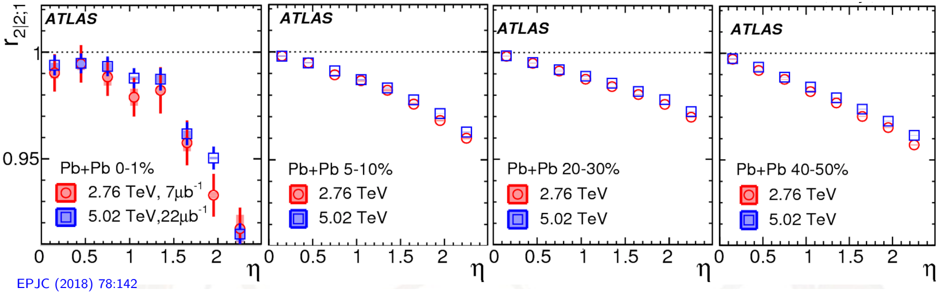

EPJC (2018) 78:142

Longitudinal flow decorrelation in Pb+Pb collisions

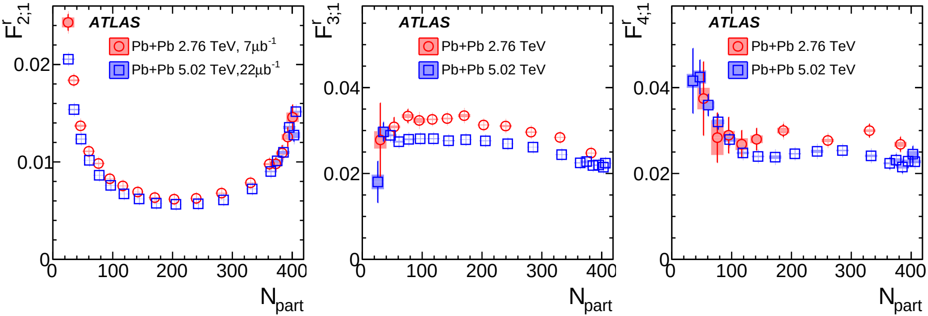

- $r_{n|n;k}(\eta)$ are expected to be approximately a linear function of η (JPhysG 44, 075106 (2017)):

$$r_{n|n;k}(\eta) \approx 1 - 2F^r_{n;k}\eta, \quad F^r_{n;k} = F^{\rm asy}_{n;k} + F^{\rm twi}_{n;k}$$

- Slope for $r_{2|2;1}$ first decrease and theen increase as a function of $N_{\rm part}$.
- Slopes for higher-order harmonics are larger.
- Decorrelation of v_n, $(n = 2, 3, 4)$ is $10 - 20\%$ stronger in 2.76 TeV than in 5.02 TeV Pb+Pb collisions.

EPJC (2018) 78:142

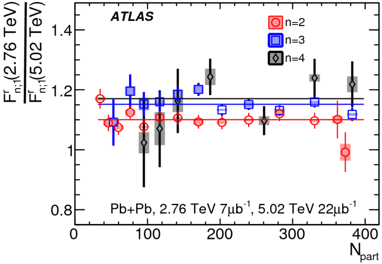

v_n – mean p_T correlations in Pb+Pb

- Correlations between magnitudes of the flow harmonics and other global event characteristics, e.g. mean p_T, $[p_\mathrm{T}]$, may provide ne insight into the properties of the QGP.
- Replace the standard Pearson's R coefficient with a modified correlator to avoid additional broadening of $\mathrm{v}_n\{2\}^2$ and $[p_\mathrm{T}]$ distributions due to finite charged particle track multiplicity (PRC 93, 044908 (2016)):

$$R = \frac{\mathrm{cov}(\mathrm{v}_n\{2\}^2, [p_\mathrm{T}])}{\sqrt{\mathrm{Var}(\mathrm{v}_n\{2\}^2)}\sqrt{\mathrm{Var}([p_\mathrm{T}])}} \Rightarrow \rho = \frac{\mathrm{cov}(\mathrm{v}_n\{2\}^2, [p_\mathrm{T}])}{\sqrt{\mathrm{Var}(\mathrm{v}_n\{2\}^2)_\mathrm{dyn}}\sqrt{c_k}}$$

- Multiplicity dependent variances are replaced by their dynamical counterparts (STAR PRC 72, 044902 (2005)):

$$c_k = \left\langle \frac{1}{N_\mathrm{pair}} \sum_{i,j\neq i} \left(p_{\mathrm{T,i}} - \langle [p_\mathrm{T}] \rangle\right)\left(p_{\mathrm{T,j}} - \langle [p_\mathrm{T}] \rangle\right) \right\rangle$$

$$\mathrm{Var}(\mathrm{v}_n\{2\}^2)_\mathrm{dyn} = \mathrm{v}_n\{2\}^4 - \mathrm{v}_n\{4\}^4 = \langle\{4\}_n\rangle - \langle\{2\}_n\rangle^2$$

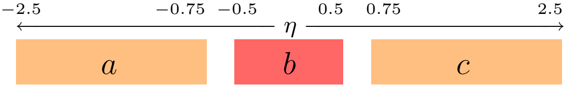

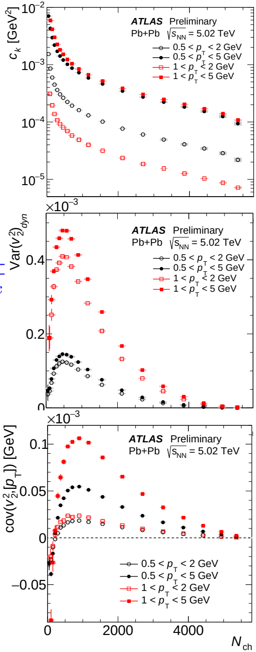

ATLAS-CONF-2018-008

v_n – mean p_{T} correlations in Pb+Pb

- Correlations between magnitudes of the flow harmonics and other global event characteristics, e.g. mean p_{T}, $[p_{\mathrm{T}}]$, may provide ne insight into the properties of the QGP.
- Replace the standard Pearson's R coefficient with a modified correlator to avoid additional broadening of $\mathrm{v}_n\{2\}^2$ and $[p_{\mathrm{T}}]$ distributions due to finite charged particle track multiplicity (PRC 93, 044908 (2016)):

$$R = \frac{\mathrm{cov}(\mathrm{v}_n\{2\}^2, [p_{\mathrm{T}}])}{\sqrt{\mathrm{Var}(\mathrm{v}_n\{2\}^2)}\sqrt{\mathrm{Var}([p_{\mathrm{T}}])}} \Rightarrow \rho = \frac{\mathrm{cov}(\mathrm{v}_n\{2\}^2, [p_{\mathrm{T}}])}{\sqrt{\mathrm{Var}(\mathrm{v}_n\{2\}^2)_{\mathrm{dyn}}}\sqrt{c_k}}$$

- Multiplicity dependent variances are replaced by their dynamical counterparts (STAR PRC 72, 044902 (2005)):

$$c_k = \left\langle \frac{1}{N_{\mathrm{pair}}} \sum_{i,j\neq i} (p_{\mathrm{T,i}} - \langle[p_{\mathrm{T}}]\rangle)(p_{\mathrm{T,j}} - \langle[p_{\mathrm{T}}]\rangle) \right\rangle$$

$$\mathrm{Var}(\mathrm{v}_n\{2\}^2)_{\mathrm{dyn}} = \mathrm{v}_n\{2\}^4 - \mathrm{v}_n\{4\}^4 = \langle\{4\}_n\rangle - \langle\{2\}_n\rangle^2$$

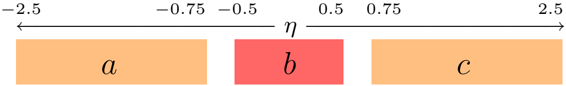

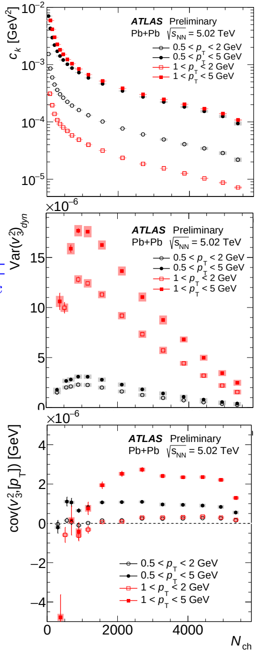

ATLAS-CONF-2018-008

v_n – mean p_T correlations in Pb+Pb

- Correlations between magnitudes of the flow harmonics and other global event characteristics, e.g. mean p_T, $[p_\mathrm{T}]$, may provide ne insight into the properties of the QGP.
- Replace the standard Pearson's R coefficient with a modified correlator to avoid additional broadening of $\mathrm{v}_n\{2\}^2$ and $[p_\mathrm{T}]$ distributions due to finite charged particle track multiplicity (PRC 93, 044908 (2016)):

$$R = \frac{\mathrm{cov}(\mathrm{v}_n\{2\}^2, [p_\mathrm{T}])}{\sqrt{\mathrm{Var}(\mathrm{v}_n\{2\}^2)}\sqrt{\mathrm{Var}([p_\mathrm{T}])}} \quad \Rightarrow \quad \rho = \frac{\mathrm{cov}(\mathrm{v}_n\{2\}^2, [p_\mathrm{T}])}{\sqrt{\mathrm{Var}(\mathrm{v}_n\{2\}^2)_\mathrm{dyn}}\sqrt{c_k}}$$

- Multiplicity dependent variances are replaced by their dynamical counterparts (STAR PRC 72, 044902 (2005)):

$$c_k = \left\langle \frac{1}{N_\mathrm{pair}} \sum_{i,j\neq i} \left(p_{\mathrm{T},\mathrm{i}} - \langle [p_\mathrm{T}] \rangle\right)\left(p_{\mathrm{T},\mathrm{j}} - \langle [p_\mathrm{T}] \rangle\right) \right\rangle$$

$$\mathrm{Var}(\mathrm{v}_n\{2\}^2)_\mathrm{dyn} = \mathrm{v}_n\{2\}^4 - \mathrm{v}_n\{4\}^4 = \langle\{4\}_n\rangle - \langle\{2\}_n\rangle^2$$

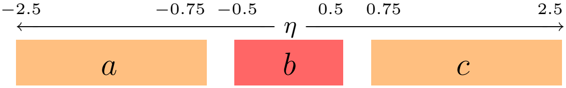

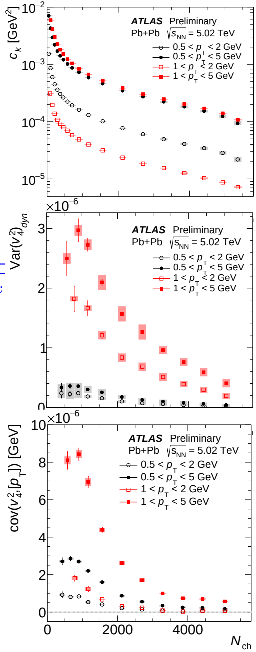

ATLAS-CONF-2018-008

v_n — mean p_T correlations in Pb+Pb

- $\rho(\mathrm{v}_2\{2\}^2, [p_\mathrm{T}])$
  - rapid increase with centrality for $N_\mathrm{part} < 100$, starting from negative values at $N_\mathrm{part} < 40$,
  - weaker increasing dependence is observed over the N_part range $100 - 350$, and a fall in more central collisions,
  - significant correlation in midcentral events is attributed to stronger hydrodynamic reponse to the large initial state eccentricities (PRC 93, 024913 (2016)).
- $\rho(\mathrm{v}_3\{2\}^2, [p_\mathrm{T}])$
  - correlations for v_3 are smaller and have a weaker centrality dependence compared to v_2,
  - correlations are positive for all studied centralities except for $N_\mathrm{part} < 100$ where they are negative or consistent with zero.
- $\rho(\mathrm{v}_4\{2\}^2, [p_\mathrm{T}])$
  - significant positive correlations over the full N_part range,
  - largest values of ρ are observed at low $N_\mathrm{part} \approx 100$, magnitude of v_3 and v_4 correlations are similar at $N_\mathrm{part} > 270$
- Theoretical predictions are consistent with the data for $\rho(\mathrm{v}_2\{2\}^2, [p_\mathrm{T}])$ and $\rho(\mathrm{v}_3\{2\}^2, [p_\mathrm{T}])$ (PRC 93, 044908 (2016))

ATLAS-CONF-2018-008

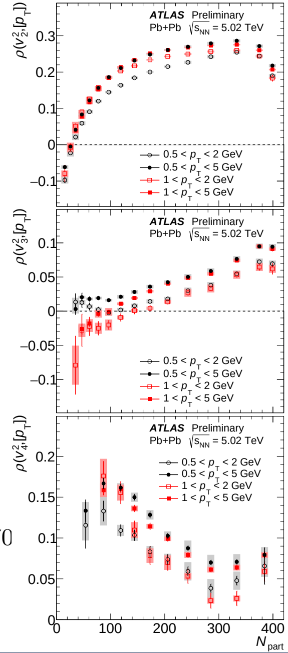

Azimuthal anizotropy in Xe+Xe collisions

- Flow harmonics, $\mathrm{v}_2 - \mathrm{v}_5$, have been measured in Xe+Xe collisions at $\sqrt{s_{\mathrm{NN}}} = 5.44$ TeV using 2PC, template fitting and SP methods as a function of p_{T} and centrality.

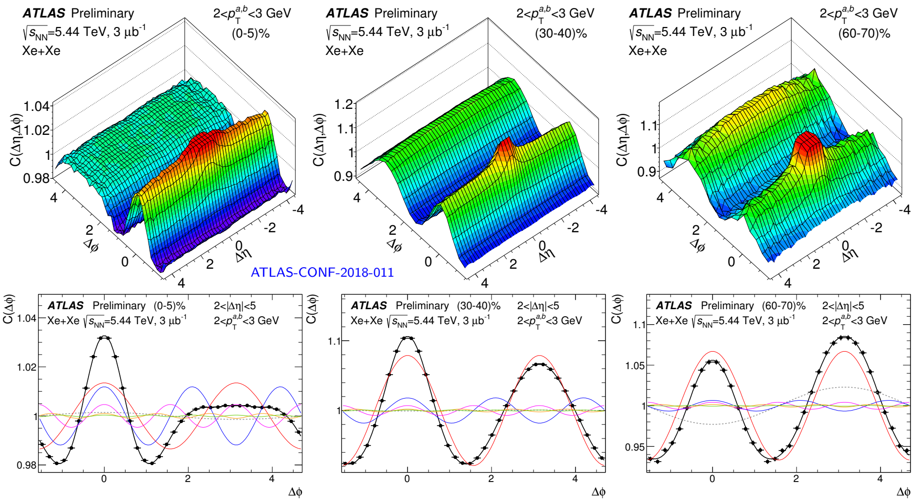

Azimuthal anizotropy in Xe+Xe collisions

- Flow harmonics, $v_2 - v_5$, have been measured in Xe+Xe collisions at $\sqrt{s_{\rm NN}} = 5.44$ TeV using 2PC, template fitting and SP methods as a function of $p_{\rm T}$ and centrality.

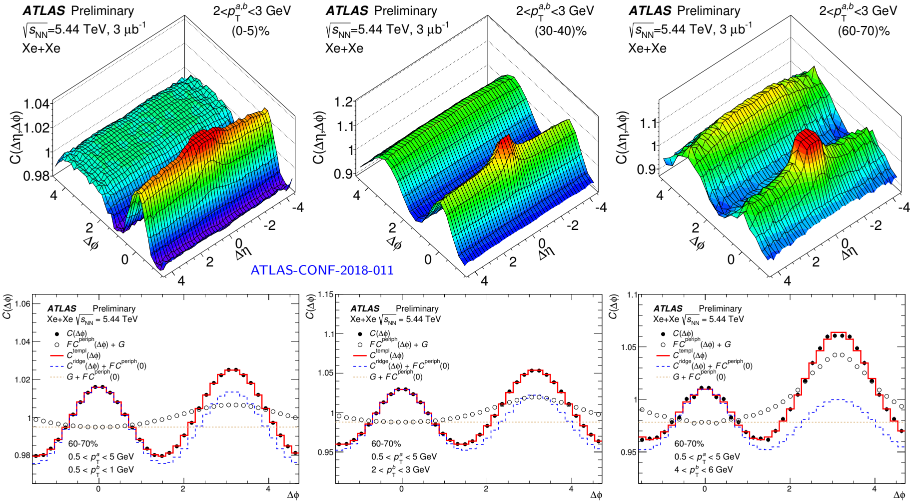

- In the template fit $C^{\rm periph}(\Delta\phi)$ is constructed using $\sqrt{s} = 5.02$ TeV pp events with less than 20 reconstructed tracks.

Event-by-event flow fluctuations in Xe+Xe collisions

- If flow fluctuations are 2D Gaussian in the transverse plane:
$$\mathrm{v}_n\{2\mathrm{PC}\} = \sqrt{\bar{\mathrm{v}}_n^2 + \delta_n^2}, \quad \mathrm{v}_n\{4\} = \mathrm{v}_n\{6\} = \bar{\mathrm{v}}_n$$
- Similar centrality dependence for different order flow cumulants, $\mathrm{v}_2\{2k\}$: largest in mid-centraland decreasing towards both central and peripheral.
- $\mathrm{v}_2\{2\mathrm{PC}\} > \mathrm{v}_2\{4\} \approx \mathrm{v}_2\{6\}$ $\Rightarrow$ flow fluctuations close to Gaussian; also strong v_3 fluctuations: $\mathrm{v}_3\{2\mathrm{PC}\} \approx 2 \cdot \mathrm{v}_3\{4\}$
- $\mathrm{v}_2\{4\}/\mathrm{v}_2\{2\mathrm{PC}\}$ - reflects the relative strength of flow fluctuations - flow fluctuations are larger in central collisions.
- $\mathrm{v}_2\{6\}/\mathrm{v}_2\{4\} \lesssim 1$ $\Rightarrow$ in mid-central Xe+Xe collisions, the non-Gaussian component is slightly larger than in Pb+Pb.

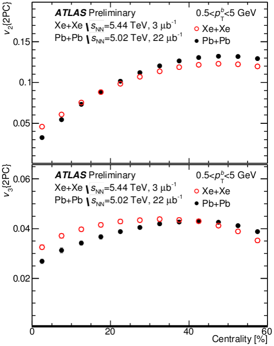

ATLAS-CONF-2018-011

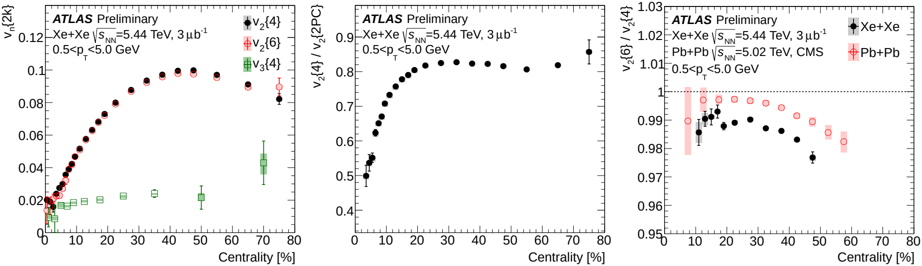

Summary

ATLAS provided several new results on correlation and fluctuations in HI collisions:

- Standard, symmetric and asymmetric cumulants have been measured with standard and subevent methods in pp, p+Pb and Pb+Pb collisions.
- Results obtained with standard method are dominated by non-flow effects. Three subevent method removes most of non-flow effects.
- Normalized cumulants show similar strength of the correlations between flow harmonics across all systems.
- Within $(1 \sim 2)\sigma$ syst. uncertainties, the Z-tagged v_2 is consistent with the min-bias v_2.
- Evidence for long-range azimuthal correlations and collectivity in small systems is confirmed and supplemented by new ATLAS measurements.
- The factorisation of two-particle azimuthal correlations into single-particle flow harmonics was found to be broken, with the magnitude of decorrelation increasing linearly with the rapidity separation between two particles.
- Significant correlations of flow harmonics with event mean-p_{T} in Pb+Pb collisions is observed.
- A comprehensive study of flow in Xe+Xe collisions at 5.44 TeV has been performed and compared to Pb+Pb at 5.02 TeV.

Thank you for your attention!

Backup slides

Heavy-ion data sets

- A+A collisions:
  - Pb+Pb @ 2.76 TeV (2011), $L_{\text{int}} = 0.14$ nb^{-1}
  - Pb+Pb @ 5.02 TeV (2015), $L_{\text{int}} = 0.49$ nb^{-1}
  - Xe+Xe @ 5.44 TeV (2017), $L_{\text{int}} = 3$ μb^{-1}
- p + A collisions:
  - p+Pb @ 5.02 TeV (2013), $L_{\text{int}} = 29$ nb^{-1}
  - p+Pb @ 5.02 TeV (2016), $L_{\text{int}} = 0.5$ nb^{-1}
  - p+Pb @ 8.16 TeV (2016), $L_{\text{int}} = 0.16$ pb^{-1}
- Reference pp samples:
  - pp @ 8 TeV (2012), $L_{\text{int}} = 19.4$ fb^{-1}
  - pp @ 2.76 TeV (2013), $L_{\text{int}} = 4$ pb^{-1}
  - pp @ 5.02 TeV (2015), $L_{\text{int}} = 28$ pb^{-1}
  - pp @ 5.02 TeV (2017), $L_{\text{int}} = 270$ pb^{-1}

The ATLAS detector

Detector coverage:

Inner Detector (ID):

$|\eta| < 2.5$

Calorimeter (CAL):

$|\eta| < 3.2$ (EM)

$|\eta| < 4.9$ (HAD)

$3.2 < |\eta| < 4.9$ (FCal)

Muon Spectrometer (MS):

$|\eta| < 2.7$

Zero Degree Cal. (ZDC):

$|\eta| > 8.3 \quad @z = \pm 140$ m

MB Trig. Scint. (MBTS):

$2.1 < |\eta| < 3.9$

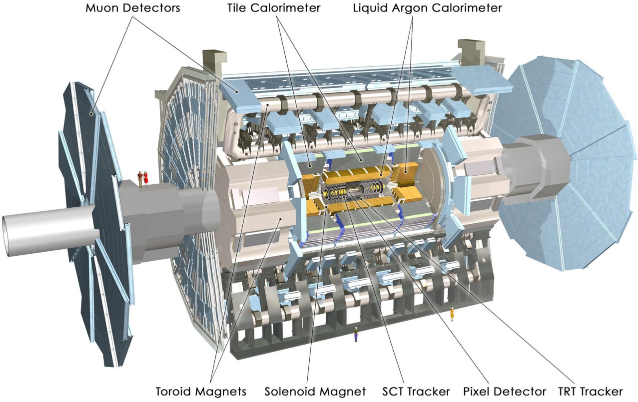

Magnetic fields:

- 2T solenoid field in ID
- Toroidal field in MS

Identification of minimum-bias p+Pb and Pb+Pb collision
measurement of spectator neutrons in ZDC and charged particle tracks (pulse hight and arrival times) in MBTS.

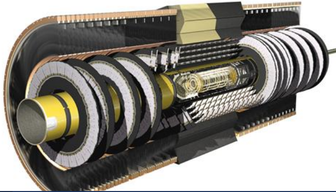

Centrality determination in Pb+Pb and p+Pb

- Centrality is measured using forward calorimeters $(3.2 < |\eta| < 4.9)$:

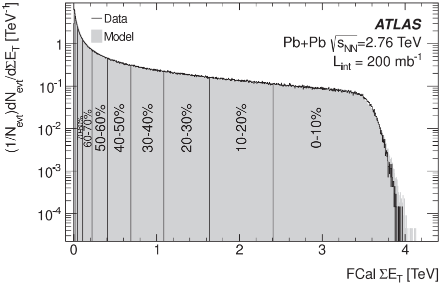

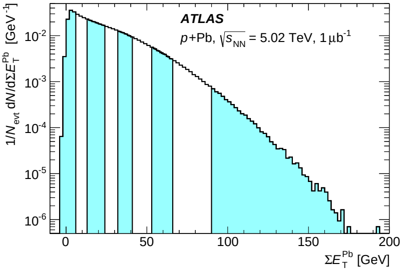

- in Pb+Pb use sum of E_{T} on both sides,
- in p+Pb use sum of E_{T} on Pb-going side only,
- for Pb+Pb use Glauber MC for geometry,
- for p+Pb use both Glauber and Glauber-Gribov color fluctuation model (PLB 633: 245 (2006)).
- Average number of participants (N_{part}) for each centrality bin resulting from fits to the measured E_{T} distribution for p+Pb.

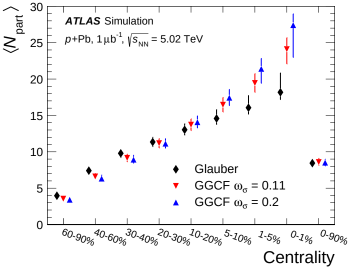

Pileup subtraction in high-luminosity pp data ($\mu \sim 20$)

- Tracks comming from pileup are partially rejected by requiring matching to the collision vertex where Z-boson is produced. Then the measured distributions are corrected for pileup on a statistical bases.
- Direct - tracks and track pairs that pass selection criteria and result from a single event.
- Direct contributions consist from Signal and from pileup interactions (Background).
- Use Mixed events constructed from tracks from different events, but with similar μ and $|(z_0^{\mathrm{trk}} - z_{\mathrm{vtx}}^{Z\text{-boson}})\sin\theta| < 0.75$ mm, to obtain Background distributions as functions of both $n_{\mathrm{trk}}^{\mathrm{mixed}}$ and $\nu \equiv \langle n_{\mathrm{trk}}^{\mathrm{bkgd}} \rangle$.
- One can build transition matrices, which can be used in the unfolding to restore $n_{\mathrm{trk}}^{\mathrm{signal}}$:

$$M(\nu, n_{\mathrm{trk}}^{\mathrm{signal}}, n_{\mathrm{trk}}^{\mathrm{direct}}) =$$
$$= P_{\mathrm{Dir}}(\nu < 0.5, n_{\mathrm{trk}}^{\mathrm{signal}}) P_{\mathrm{Mix}}(\nu, n_{\mathrm{trk}}^{\mathrm{direct}} - n_{\mathrm{trk}}^{\mathrm{signal}})$$

ATLAS-CONF-2017-068

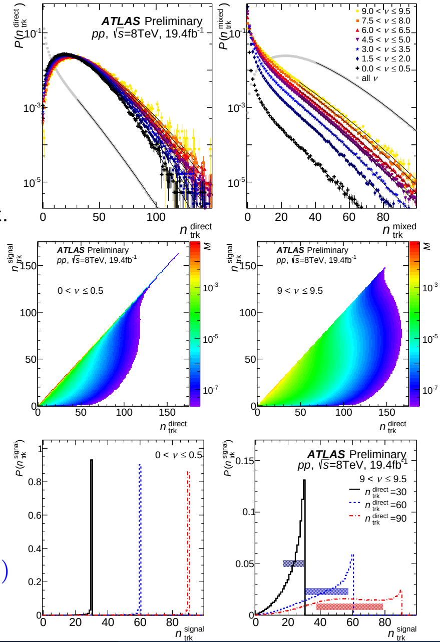

Pileup correction for the pair-distribution

- D=Direct, S=Signal, B=Bkgd

$$D^a \times D^b \equiv \sum_{a \in D} \sum_{b \in D, b \neq a} (\phi^a - \phi^b)$$

- $D^a \times D^b = S^a \times S^b +$
  $+ S^a \times B^b + B^a \times S^b + B^a \times B^b$

- Averaging over many events:

$$\langle S^a \times S^b \rangle = \langle D^a \times D^b \rangle - \langle B^a \times B^b \rangle - \\ - \langle B^a \times S^b \rangle - \langle S^a \times B^b \rangle$$

- S and B are independent, and $\langle S^a \rangle = \langle D^a \rangle - \langle B^a \rangle$, hence

$$\langle S^a \times S^b \rangle = \langle D^a \times D^b \rangle - \langle B^a \times B^b \rangle - \\ - \langle D^a \rangle \times \langle B^b \rangle - \langle B^a \rangle \times \langle D^b \rangle + \\ + 2 \langle B^a \rangle \times \langle B^b \rangle$$

- Background events are statistically equivalent to M=Mixed events at the same multiplicity.

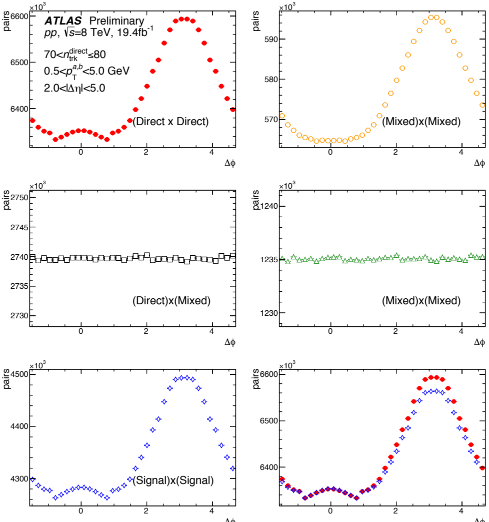

ATLAS-CONF-2017-068

$$\left(S^a \times S^b\right)\Big|^{n_{\mathrm{trk}}^{\mathrm{signal}} = n_{\mathrm{trk}}^{\mathrm{signal},0}} = \sum_{\nu}^{\nu^{\max}} \sum_{n_{\mathrm{trk}}^{\mathrm{direct}} = n_{\mathrm{trk}}^{\mathrm{signal},0}}^{n_{\mathrm{trk}}^{\mathrm{direct,max}}} \left(P(n_{\mathrm{trk}}^{\mathrm{signal}}) N_{\mathrm{events}}^{\mathrm{direct}} \langle S^a \times S^b \rangle \right)\Big|_{\nu - (\nu + 0.5)}^{n_{\mathrm{trk}}^{\mathrm{direct}}}$$

$D^\star$ meson production in p+Pb collisions

- Heavy quarks are primarily produced at early stages of HI collisions in gluon-gluon fusion and can carry information about early stage properties of the QGP.
- Compared with gluons and light quarks, heavy quarks lose less energy when traversing the medium due to the dead-cone effect (JPhys G17 (1991) 1481).
- Reconstruction of $D^\star$ mesons in "golden channel":

$$D^{\star +} \rightarrow D^0 \pi^+_{\rm slow} \rightarrow (K^- \pi^+)\pi^+_{\rm slow} + C.C.$$

- D^0 candidates are constructed from opposite-sign pairs of tracks with $p_{\rm T} > 1$ GeV each.
  Both combinations of kaon and pion masses are considered for the tracks, since no particle identification is applied.
  The invariant mass of the pair is required to be in the range $1.75 < m(K\pi) < 1.96$ GeV.
- $D^\star$ candidates are built by adding a soft pion track with $p_{\rm T} > 250$ MeV to D^0 candidates.

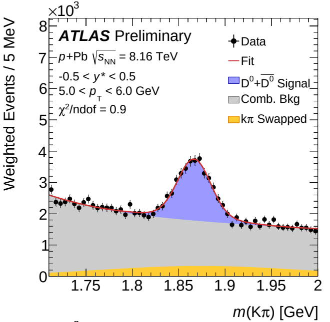

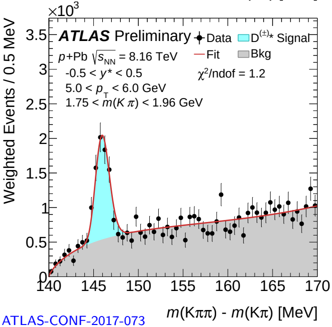

ATLAS-CONF-2017-073

$D^{\star}$-hadron correlations in p+Pb collisions

- Study of azimuthal angular correlations between charged particles and inclusive $D^{\star}$ candidates with $3 < p_{\mathrm{T}} < 30$ GeV and $-1.5 < y^{\star} < 0.5$ in p+Pb collisions.
- $D^{\star}$-hadron ($D^{\star}$-h) correlations are quantified using the two-particle correlation function $C(\Delta\phi)$ obtained from all pairs of $D^{\star}$ candidates and charged particle tracks, separated in pseudorapidity by $\Delta\eta > 1$.
- A template fitting method is used to extract the harmonic coefficients associated with the long-range ridge contribution, using the shape of peripheral contribution obtained from events with low multiplicity of $10 < N_{\mathrm{ch}} < 80$.
- A finite $\mathrm{v}_{2,2}$ is extracted from inclusive $D^{\star}$-h correlations with $(1 \sim 2)\sigma$ significance.

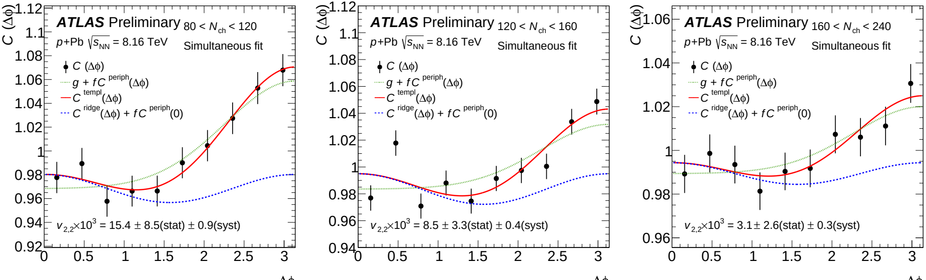

ATLAS-CONF-2017-073

v_n measured by the SP method in Xe+Xe collisions

- Scalar Product (SP) method for v_n calculation:

$$v_n\{\mathrm{SP}\} = \Re \frac{\langle q_n^N Q_n^{P\star}\rangle}{\sqrt{\langle Q_n^N Q_n^{P\star}\rangle}}$$

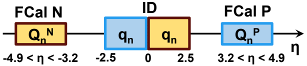

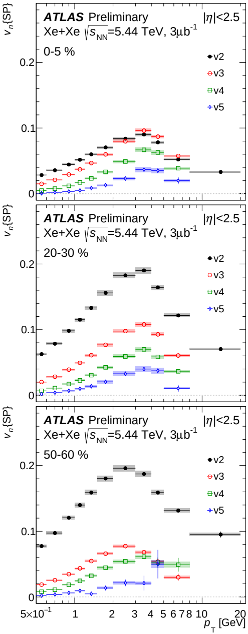

- For all centralities, $v_n\{\mathrm{SP}\}(p_{\mathrm{T}})$ increase at low p_{T}, reach a maximum at $2-4$ GeV and then decrease.
- As a function of centrality, the v_n values for all harmonics are comparable for Xe+Xe and Pb+Pb $\Rightarrow$ flow is related to the initial geometry rather than to the number of sources.
- Difference between v_n as a function of N_{part} may be related to the difference of sizes of ${}^{129}_{54}\mathrm{Xe}$ and ${}^{208}_{82}\mathrm{Pb}$ nuclei.

ATLAS-CONF-2018-011

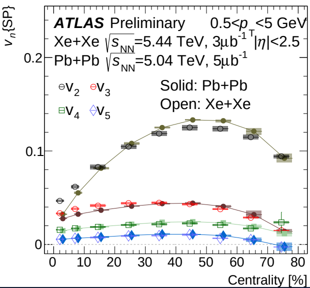

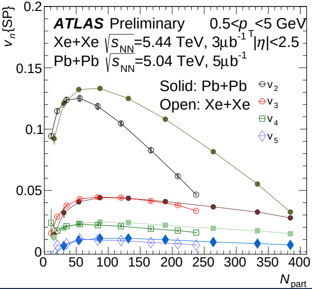

Symmetric and asymmetric cumulants in Xe+Xe collisions

- Differential flow cumulant, $\mathrm{v}_n\{4\}(p_\mathrm{T})$, is calculated as:

$$\mathrm{v}_n\{4\} = -\frac{d_n\{4\}}{(-c_n\{4\})^{3/4}}, \quad d_n\{4\} = \langle d\{4\}_n\rangle - 2\langle d\{2\}_n\rangle\langle\{2\}_n\rangle$$

- For all centralities, $\mathrm{v}_2\{4\}(p_\mathrm{T})$ and $\mathrm{v}_3\{4\}(p_\mathrm{T})$ increase at low p_T, reach a maximum at $2-4$ GeV and then decrease.
- $\mathrm{sc}_{2,3}$ and $\mathrm{sc}_{2,4}$ $\Rightarrow$ v_2 and v_3 are anti-correlated, and positive correlation between v_2 and linear component of v_4.
- $\mathrm{nsc}_{n,m}$ and $\mathrm{nac}_{n,m}$ keep increasing towards peripheral, i.e. their centrality dependence originates mainly form the $\langle \mathrm{v}_n^2\rangle$.

ATLAS-CONF-2018-011